THE ASTROPHYSICAL JOURNAL, 557:560–572, 2001 August 20

ON THE NONTHERMAL EMISSION AND ACCELERATION OF ELECTRONS IN COMA AND OTHER CLUSTERS OF GALAXIES

VAHÉ PETROSIAN
Astronomy Program and Departments of Physics and Applied Physics, Center for Space Science and Astrophysics, Stanford University, Stanford, CA 94305; vahe@astronomy.stanford.edu
Received 2001 January 19; accepted 2001 March 21

ABSTRACT

Some clusters of galaxies, in addition to thermal bremsstrahlung (TB), emit detectable diffuse radiation from the intracluster medium (ICM) at radio, EUV, and hard X-ray (HXR) ranges. The radio radiation must be due to synchrotron by relativistic electrons, and the inverse Compton scattering by the cosmic microwave background radiation of the same electrons is the most natural source for the HXR and perhaps the EUV emissions. However, simple estimates give a weaker magnetic field than that suggested by Faraday rotation measurements. Consequently, nonthermal bremsstrahlung (NTB) and TB have also been suggested as sources of these emissions. We show that NTB cannot be the source of the HXRs (except for a short period) and that the difficulty with the low magnetic field in the IC model is alleviated if the effects of observational selection bias, nonisotropic pitch angle distribution, and spectral breaks in the energy distribution of the relativistic electrons are taken into account. From these considerations and the strength of the EUV emission, we derive a spectrum for the radiating electrons and discuss possible acceleration scenarios for its production. We show that continuous and in situ acceleration in the ICM of the background thermal electrons is difficult and requires unreasonably high energy input. Similarly, acceleration of injected relativistic electrons, say, by galaxies, seems unreasonable because it will give rise to a much flatter spectrum of electrons than required, unless a large fraction of energy input is carried away by electrons escaping the ICM, in which case one obtains EUV and HXR emissions extending well beyond the boundaries of the diffuse radio source. A continuous emission by a cooling spectrum resulting from interaction with ICM of electrons accelerated elsewhere also suffers from similar shortcomings. The most likely scenario appears to be an episodic injection acceleration model, whereby one obtains a time-dependent spectrum that for certain phases of its evolution satisfies all the requirements.

Subject headings: acceleration of particles — galaxies: clusters: general — galaxies: clusters: individual (Coma) — magnetic fields — X-rays: galaxies: clusters

1. INTRODUCTION

The most prominent radiation from the intracluster medium (ICM) of clusters of galaxies is the thermal bremsstrahlung (TB) or free-free emission in the soft X-ray (SXR; 2–10 keV) region, which can reach a luminosity $L_{\rm SXR} \sim 10^{45}$ ergs s^{-1} and implies gas temperatures of $T \sim 10^8$ K and emission measures of EM $\sim 10^{68}$ cm^{-3} (density $n \sim 10^{-3}$ cm^{-3}, radius $R \sim 1$ Mpc). For the Coma Cluster $L_{\rm SXR} \simeq 5 \times 10^{44}$ and $kT = 8.2$ keV. There is, however, growing evidence for significant nonthermal activity in some clusters. The first of these to be discovered in just a few clusters, notably in the Coma Cluster (for the most recent observations see Giovannini & Feretti 2000), was the diffused (so-called halo) radio emission of luminosity $L_R \sim 10^{41}$ ergs s^{-1} in the frequency range 30 MHz $< \nu <$ 4 GHz, whose source must be synchrotron radiation by relativistic electrons. The range and distributions of the Lorentz factor γ of these electrons and their total energy depend on the strength, geometry, and distribution of the magnetic field B. The field is measured by Faraday rotation to be a few μG in some clusters that would require electrons with $\gamma > 10^3$. The exact source of these electrons is still a matter of considerable debate. For a review see Eilek (1999), Giovannini et al. (1993), Kim et al. (1990), and references therein to earlier works. More recently, radiation (most likely nonthermal in origin) has been discovered in the form of excess flux at low and high ends of the thermal radiation in several clusters. The *Extreme Ultraviolet Explorer* (*EUVE*), with the passband of 69–245 eV, has detected excess radiation from Coma (Lieu et al. 1996b). The luminosity of this soft excess radiation in the 0.07–0.4 keV range is $L_{\rm EUV} \sim 2 \times 10^{43}$ ergs s^{-1} (Lieu et al. 1999). Similarly, *BeppoSAX* and *Rossi X-Ray Timing Explorer* (*RXTE*) have detected excess hard X-ray (HXR) radiation in the 20–80 keV range from Coma (Fusco-Femiano et al. 1999; Rephaeli, Gruber, & Blanco 1999), A2256 (Fusco-Femiano et al. 2000), and possibly A2199 (Kaastra et al. 1999). The luminosity of Coma in this range is $L_{\rm HXR} \sim 4 \times 10^{43}$ ergs s^{-1}. The EGRET instrument on board the *Compton Gamma-Ray Observatory* (*CGRO*) sets an upper limit of $L_{\gamma\text{-ray}} \lesssim 10^{43}$ ergs s^{-1} above 100 MeV (Sreekumar et al. 1996). These observations are summarized in Table 1 and assume a Hubble constant of 60 km s^{-1} Mpc^{-1}.

Initially the excess EUV radiation was explained in terms of one or more cooler thermal components (Lieu et al. 1996a, 1996b; Mittaz, Lieu, & Lockman 1998), but soon after, a nonthermal process, namely, the inverse Compton (IC) scattering by the cosmic microwave background (CMB) radiation of electrons with energies about 10 times smaller than those responsible for the radio emission, was proposed as the source of the EUV radiation by many authors (Hwang 1997; Enßlin & Biermann 1998; Bowyer & Berghöfer 1998; Lieu et al. 1999). The initial interpretation of the HXR excess was also based on the IC model (Fusco-Femiano et al. 1999; Sarazin & Lieu 1998). This seems to be a natural explanation since electrons with energies very

TABLE 1

SUMMARY OF OBSERVATIONS

Radiation	Radio	EUV	SXR	HXR
Range	0.03–4[a]	0.07–0.4[b]	2–10[b]	20–80[b]
Spectrum	Broken power law	Uncertain	Exponential	Power law
Index (or temperature)	~ 1 and ~ 2, exponential tail	$\sim 3/2$, $kT \sim 2$[b]	$kT = 8.5^{+0.6}_{-0.5}$,[b,c] $kT = 7.51 \pm 0.18$[b,d]	0.7–6,[c] 2.35 ± 0.45[d]
Luminosity (ergs s^{-1})	10^{41}	2×10^{43}	5×10^{44}	4×10^{43}
Mechanism	Synchrotron	IC (TB)	TB	IC (NTB)

[a] In GHz.
[b] In keV.
[c] Fusco-Femiano et al. 1999.
[d] Rephaeli et al. 1999.

similar to those producing the synchrotron emission are required. In fact, long before these discoveries, strong upper limits on the nonthermal X-ray emission were set based on the IC model and the radio observations (Schlickeiser, Sievers, & Thiemann 1987).

There is, however, a major difficulty with both of these interpretations (Bowyer & Berghöfer 1998; Fusco-Femiano et al. 1999; Rephaeli et al. 1999). This is due to the simple fact that the ratio of the IC to synchrotron luminosities is equal to the ratio of the CMB to magnetic field energy densities, which for $T_{\rm CMB} = 3$ K is $15/(B/\mu G)^2$. The observed ratio of HXR to radio luminosities of about 4×10^2 implies a field strength $B < 0.2$ μG, which is much smaller than B values of several μG deduced from Faraday rotation (Eilek 1999) and equipartition of magnetic and relativistic particle energies. Comparison of the EUV and radio fluxes can also set a limit on the magnetic field, but here the limit is somewhat higher ($B \lesssim 1$ μG; Hwang 1997; Enßlin & Biermann 1998) and less reliable because it is sensitive to the uncertain extrapolation of the electron spectrum over a decade (Bowyer & Berghöfer 1998; Atoyan & Volk 2000). Because of this discrepancy, several workers have proposed nonthermal bremsstrahlung (NTB) as the source of the observed HXRs (Enßlin, Lieu, & Biermann 1999; Sarazin & Kempner 2000; Blasi 2000). However, this explanation also suffers from a major flaw because it requires a large input of energy in the ICM whose consequences have not been detected. This flaw is based on the simple fact that bremsstrahlung is an inefficient mechanism.

In the next section we describe some details of the characteristics of the ICM plasma and the constraints they put on the models. We discuss in § 3 the emission process and in § 4 the related aspect of the particle acceleration. A brief summary is presented in § 5.

2. GENERAL DESCRIPTION OF THE PROBLEM

In order to illustrate the difficulties faced in the above models, in Figure 1 we show the energy loss timescales, $\tau_{\rm loss} = -E/\dot{E}_{\rm loss}$, as a function of particle kinetic energy for all the relevant processes in this problem. Here and in what follows, unless explicitly expressed, all energies and loss rates will be in units of rest mass energy of electron $m_e c^2$, so the Lorentz factor is $\gamma = E + 1 = (1 - \beta^2)^{-1/2}$. We use the following expressions for the loss rates:

$$-\dot{E}_{\rm IC} = \frac{32\pi}{9} r_0^2 c\beta^2\gamma^2 u_{\rm ph} = 2.04 \times 10^{-20}\beta^2\gamma^2\left(\frac{T_{\rm CMB}}{3\ {\rm K}}\right)^4 {\rm s}^{-1}, \quad (1)$$

$$-\dot{E}_{\rm synch} = \frac{4}{9} r_0^2 c\beta^2\gamma^2 B^2 = 1.32 \times 10^{-21}\beta^2\gamma^2\left(\frac{B}{\mu{\rm G}}\right)^2 {\rm s}^{-1}, \quad (2)$$

$$-\dot{E}_{\rm Coul} = \frac{4\pi r_0^2 cn \ln\Lambda}{\beta} = 1.20 \times 10^{-15}\left(\frac{n/10^{-3}\ {\rm cm}^{-3}}{\beta}\right) {\rm s}^{-1}, \quad (3)$$

$$-\dot{E}_{\rm brem} = \frac{16}{3} \alpha r_0^2 cn\beta\gamma\chi(E) = 9.29 \times 10^{-20}\left(\frac{n}{10^{-3}\ {\rm cm}^{-3}}\right)\beta\gamma\chi(E)\ {\rm s}^{-1}, \quad (4)$$

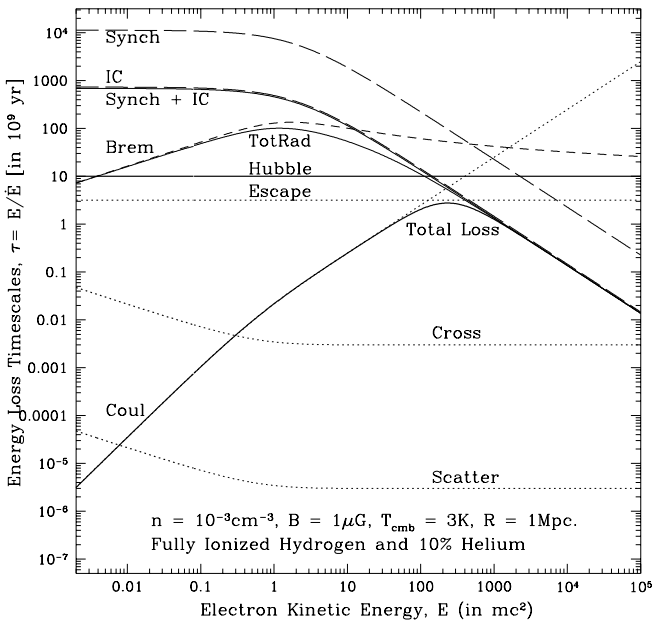

FIG. 1.—Energy loss timescales vs. energy for the four relevant interactions of electrons for typical ICM conditions. The three solid lines, from top to bottom, are for the combined synchrotron and IC, the three radiative processes, and all losses, respectively. The dotted lines show the average crossing time $T_{\rm cross} \sim R/(c\beta)$ across a region of size $R \sim 1$ Mpc, the scattering time $\tau_{\rm scat} \sim \lambda_{\rm scat}/(c\beta)$ for a constant scattering mean free path $\lambda_{\rm scat}$, and the escape time $T_{\rm esc} \sim T^2_{\rm cross}/\tau_{\rm scat}$. Note that all loss times are shorter than the Hubble time (*thick solid line*, for Hubble constant of 100 km s^{-1} Mpc^{-1}) and much longer than the electron crossing time except at low ($E < 200$ keV) and very high ($E > 200$ GeV) energies.

where α is the fine-structure constant and u_{ph} is the soft photon energy density. The IC losses are evaluated assuming the CMB with a temperature of 3 K as the source of the soft photons. The synchrotron losses are evaluated for an isotropic pitch angle distribution, and the Coulomb logarithm $\ln\Lambda$ is set to 40, a representative value for the ICM conditions. For the Coulomb and bremsstrahlung losses we assume the presence of 10% (by number) of fully ionized helium. The bremsstrahlung rate also depends on the complicated function $\chi(E)$, which is equal to 1 in the nonrelativistic limit and equals $\frac{3}{4}[\ln(2E) - \frac{1}{3}]$ at extreme relativistic energies. (For $E \gg \alpha^{-1}$ the slow varying term in the square brackets tends to the constant value of about 5.) The bremsstrahlung rate used in Figure 1 is calculated from the more exact expression given by the formula 4BN of Koch & Motz (1959).

Several immediate conclusions can be drawn from Figure 1. The lifetimes of electrons with energies in the range 200 keV $\leq E \leq$ 200 GeV are longer than the free crossing time of the electrons across the cluster (or the "mean free paths," $\lambda_{loss} = c\beta\tau_{loss} \lesssim 1$ Gpc, are much larger than the size $R \sim 1$ Mpc of the cluster). Therefore, these electrons, if unhindered, e.g., by chaotic magnetic fields or other scattering agents, will escape the cluster before losing most of their energy, and while in the cluster they will radiate what is commonly referred to as a *thin target* spectrum. The escaping electrons will radiate most of their energy outside the cluster, presumably by IC scattering of the CMB photons. This will disagree with the observations and will require a higher rate of energy input than for electrons outside the above energy range that lose all their energy before escape and develop a so-called *cooling spectrum*, giving rise to a *thick target* photon spectrum. Therefore, if all electrons were to lose all their energy in the cluster, they must be trapped efficiently so that they traverse a gigaparsec in the ICM. This can come about by a thousand reversals of the magnetic field lines or a million random scatterings of the electrons. *Hence, we require the presence of scattering agents (e.g., plasma turbulence) with a scattering mean free path $\lambda_{scat} \sim 1$ pc, or a chaotic field structure with a scale $B/\Delta B$ between 1 kpc and 1 pc.* In such a case, the electrons with energies away from the peak energy E_p of the total loss time curve at about 100 MeV diffuse through only a distance of $\lambda_{eff} \sim (\lambda_{loss}\lambda_{scat})^{1/2} \ll R$ before they lose most of their energy. This means that for production of a smooth diffuse radiation throughout the cluster *we need in situ acceleration of the electrons throughout the ICM* and cannot rely on injection of accelerated electrons into the ICM from a single source or sources separated by a distance $\gg \lambda_{eff}$. This last condition is required for electrons with 200 GeV $< E <$ 200 keV even in the absence of scattering agents. (Berezinky, Blasi, & Ptuskin [1997] address the issue of the confinement of the nonthermal particles using the scattering mean free path given by Schlickeiser et al. [1987]. However, their discussion is applicable only to protons and other ions because they ignore radiative and other losses. As evident from Figure 1 this cannot be the case for electrons.) We will return to these requirements in § 4 dealing with the acceleration process.

On the other hand, because the lifetimes at all energies are much shorter than the age of the universe, then unless the observed nonthermal radiations are short-lived transient phenomena, the acceleration of the nonthermal electrons must be continuous over the lifetime of the clusters.

Finally, we note that for $B < 1$ μG, the synchrotron process has little influence on the dynamics (acceleration and cooling) of the nonthermal electrons. It acts only as the radio emission process.

3. EMISSION PROCESSES

In this section we describe the difficulties faced in some of the proposed radiation mechanisms and derive a spectrum for the nonthermal electrons.

3.1. *Nonthermal Bremsstrahlung Emission*

Enßlin et al. (1999) were the first to propose NTB emission as the source of the observed HXR flux from clusters, whereby electrons of comparable or slightly larger energies produce the 20–80 keV radiation. Sarazin & Kempner (2000) evaluated bremsstrahlung spectra using various accelerated electron spectra and detailed bremsstrahlung cross sections. Blasi (2000) gives a combined description of the stochastic acceleration and bremsstrahlung radiation. However, all these works ignore the huge energy problem associated with this model. As is evident from Figure 1, the main difficulty of this model is the inefficiency of the bremsstrahlung process compared to the collisional losses for $E < 1$ GeV and relative to IC losses for $E > 10$ MeV. In particular, for the energy range of interest here (from 20 to $\sim$1000 keV), the ratio of the bremsstrahlung to Coulomb loss rates is less than 10^3. As shown by Petrosian (1973), the yield of the bremsstrahlung photon is a well-defined quantity independent of many unknowns of the models. For a nonrelativistic electron of initial energy E_{in} that loses all its energy (thick target case) this yield is $Y_{brem} = (4/3\pi)(\alpha/\ln\Lambda)E_{in} = 7.7 \times 10^{-5}E_{in}$ (this yield is larger by a factor of 2 for electrons losing a small fraction of their energy in the source region, the thin target case). For a power-law distribution of electrons [$N(E) \propto E^{-p}$, for $E > E_{in}$], the above expression is modified by a factor of order unity. The yield of electrons with energies between E_{in} and E_f will depend on p. For $p \sim 3.5$ required by this model this factor is 1.3 (see eq. [31] in Petrosian 1973, where $\delta + 1 = p$). This expression is also valid for relativistic energies within a factor of the order of $\ln E_{in}$ as indicated by the slow decline of the τ_{brem} curve in Figure 1 at high energies.

A yield of $Y_{brem} < 3 \times 10^{-6}$ in the 20–80 keV range means that, independent of most details of the acceleration or emission model, a large amount of energy ($L_{in} = L_{HXR}/Y_{brem} \sim 10^{49}$ ergs s^{-1}) is fed into the background plasma. If the ICM plasma were to cool only radiatively (free-free emission), at the very slow rate of $L_{ff} = 1.45 \times 10^{-23}$ ergs s^{-1} $(T/10^8\ \mathrm{K})^{1/2}(\mathrm{EM}/10^{68}\ \mathrm{cm}^{-3})$, then such an input of energy would increase its temperature at the rate of $dT/dt = L_{in}/3Nk \gtrsim 10^{-7}$ K s^{-1}. As a result the ICM temperature will exceed 10^8 K after a short time of 3×10^7 yr and will exceed 10^{10} K in a Hubble time! This, of course, is not acceptable because it will evaporate the ICM plasma into the general intergalactic medium. Either only one part in 10^4 or 10^5 of the observed HXR flux is due to the NTB process or the NTB emission phase at the observed rate is a short-lived phenomenon. Blasi (2000a) finds that his acceleration model indeed requires a similar (though somewhat smaller) rate of input of energy into the turbulence needed for acceleration and that the duration of NTB emission satisfying the observation is around several hundred million years.

The situation is very similar in what one may call the inverse bremsstrahlung model, whereby accelerated protons interacting with the background thermal electrons produce the HXRs. In the rest frame of an accelerated proton of energy $E_p = (m_p/m_e)E_e$, the process is identical to that of bremsstrahlung by accelerated electrons of energy E_e. Thus, HXRs of energy 20–200 keV can be produced by nonthermal protons of energy 40–1000 GeV. However, here again most of the proton energy will go into heating the electrons by inelastic Coulomb or Rutherford scattering. In addition, the higher energy nonthermal protons may lose some of their energy to π^0 production, which decay into 50–100 MeV gamma rays.

The presence of thermal SXR and nonthermal HXR (also nonthermal synchrotron radio) emission in the clusters is very similar to that observed in solar flares. Except in solar (and most likely in other stellar) flares the SXR flux is 10^5–10^6 times larger than the HXR flux in agreement with the above yields. In analogy to flares one may consider that acceleration of electrons is taking place in high-density magnetic loops associated with the disks or halos of, say, a thousand galaxies, each receiving 10^{45} ergs s^{-1}. The current observations do not have the spatial resolution to distinguish the ICM emission from that of many galaxies. Since the radiative equilibrium temperature $T \propto [L_{\rm in}/(Y_{\rm brem}\,{\rm EM})]^2$, a lower temperature of about 10^9 K will result for $L_{\rm in} \sim 10^{45}$ ergs s^{-1}, density $n \sim 0.1$, and a region of size $L \sim 30$ kpc. [Actually, for this size scale conduction losses $L_{\rm cond} \sim 2 \times 10^{45}(T/10^8\ {\rm K})^{3.5}(L/30\ {\rm kpc})$ become comparable and exceed the radiative losses for $T \geq 10^8$ K so that the temperature never exceeds the latter value.] In any case such hot galactic plasmas will evaporate into the ICM and may be the source of the hot SXR-emitting gas. Only a small fraction (less than 0.01%) of the energy can go into the ICM plasma. Most of it must be dissipated in the galaxies. It is not obvious how the effects of such an energy input, which is much larger than that from stellar sources (stellar winds, supernovae, and other explosions), can be hidden.

Therefore, we conclude that the main objection to the NTB emission is very robust; it is essentially determined by the values of the fine-structure constant and the Coulomb logarithm and very difficult to circumvent. This leads to the conclusion that for all three clusters, Coma, A2256, and A2199, *the NTB emission from ICM as a source of the observed HXRs is not tenable, unless it is a short-lived* (*less than* 10^8 *yr*) *phenomenon.*

A corollary of this is that one can put a strong constraint on the spectrum and energy density of the nonthermal electrons below the peak energy $E_p \sim 100$ MeV where the elastic Coulomb collision losses are larger than the radiative losses. As we will show below, the spectral distribution of the electrons below this energy must be flatter than $E^{-1/2}$ or there must exist a sharp cutoff below several MeV.

3.2. *Inverse Compton Emission*

As can be seen from Figure 1, for typical ICM conditions, the IC emission exceeds bremsstrahlung for $E > 10$ MeV. However, as already pointed out by many of the authors cited in § 1, this model also suffers from the inefficiency of the IC radiation relative to the synchrotron radiation. The relative flux of these two radiations depends on the CMB photon density, which is known accurately, and on the value of the magnetic field, which is not so well known. From equations (1) and (2) the ratio of these fluxes can be obtained to be roughly equal to

$$\frac{\dot{E}_{\rm IC}}{\dot{E}_{\rm synch}} = 19.8\left(\frac{T_{\rm CMB}}{2.8\ {\rm K}}\right)^4\left(\frac{\mu{\rm G}}{B}\right)^2 . \quad (5)$$

The most reliable measures of ICM B field come from the Faraday rotation of the background radio sources. In the cores of several well-studied clusters, values of several μG have been derived (Eilek 1999). Furthermore, the measured values refer to the net line-of-sight component so that for a chaotic field the actual value could be even larger. This is in apparent contradiction with the value $B \sim 0.2$ μG one deduces from the observed ratio of the HXR to radio fluxes, which is about 500. Actually, the observed Faraday rotation in the Coma Cluster gives a value of $B \sim 0.3$ μG for an ordered magnetic field and a larger value of $B \sim 2$ μG if the field is chaotic on the scale of several tens of kiloparsecs (Kim et al. 1990; Ferretti et al. 1995). Estimates based on the assumption of energy equipartition between nonthermal electrons, protons, and magnetic field give $B \sim 1$ μG. The radio properties are somewhat different for A2256, but the same kind of discrepancy seems to be present for this cluster as well (Fusco-Femiano et al. 2000). However, there is no Faraday rotation data for this cluster, so the argument against the IC model is not as strong here. The detection of HXR flux in A2199 is generally considered as marginal, which combined with the absence of a detectable halo radio source or Faraday rotation makes conclusions based on this cluster less reliable.

However, in comparison with the insurmountable difficulty of the NTB model, there are possible ways to avoid the problems of the IC model. Below we describe several effects that alleviate these problems. We will use the Coma Cluster for quantitative discussion.

3.2.1. *Selection Effects*

The low value of the B field in clusters with observed HXR emission can be simply an observational selection effect. For a given radio flux of the halo source and independent of any equipartition argument, clusters with lower B values will have the stronger IC flux and therefore will be more readily detected by *BeppoSAX* and *RXTE* (or *EUVE* if electron spectrum extends to lower energies). Unfortunately, the numbers of known clusters with either a halo radio source, HXR emission, or both are too small to make any reliable quantitative estimates of the effects of this selection bias.

A related and similar effect can arise if the distributions of the magnetic field and relativistic electrons are inhomogeneous and anticorrelated. In this case the radio and IC emissions will come mainly from weak-field regions while the Farady rotation is determined by the average field. Even in the absence of such an anticorrelation, there are other subtle effects arising from spatial inhomogeneities that can give rise to a discrepancy between the magnetic field strengths based on the IC emission and the Faraday rotation measure (Goldshmidt & Rephaeli 1993). Explorations of spatially inhomogeneous models are beyond the scope of this paper.

3.2.2. *Complex Electron Spectra*

The estimate of the ratio of IC to synchrotron emission based on equation (5) is for a monoenergetic electron. For a spectrum of accelerated electrons this relation is somewhat more complex. However, for a power-law distribution of

accelerated electrons with index p one obtains similar constraints on the value of the magnetic field using the observed HXR and radio fluxes. Using the well-known expression for the spectra of IC and synchrotron emissions, it can be shown that the ratio of the HXR photon flux (in units of photons s^{-1} cm^{-2} keV^{-1}) at photon energy ϵ to the radio flux (in Jy units) at frequency ν is

$$R = \frac{f_{\rm IC}(\epsilon)}{f_{\rm synch}(\nu)} = 1.86 \times 10^{-8} \left(\frac{\text{photons}}{\text{s cm}^2 \text{ keV Jy}}\right) \times \left(\frac{\epsilon}{20 \text{ keV}}\right)^{-\alpha} \left(\frac{\nu}{\text{GHz}}\right)^{\alpha-1} \times \left(\frac{T_{\rm CMB}}{2.8 \text{ K}}\right)^{\alpha+2} \left(\frac{B_\perp}{\mu\text{G}}\right)^{-\alpha} g(p) , \quad (6)$$

where $\alpha = (p + 1)/2$ is the IC photon spectral index and $g(p)$ is a complicated function of index p that is equal to 11.0, 41.2, 181, and 755 for $p = 2$, 3, 4, and 5, respectively (see eqs. [6.36] and [7.29] of Rybicki & Lightman 1979). In this range of p a good approximation to use is $g(p) = e^{1.42p-0.51}$. Using this approximation, it can be shown that

$$\frac{B_\perp}{\mu\text{G}} = \left(\frac{20 \text{ keV}}{\epsilon}\right) \left(\frac{\nu}{\text{GHz}}\right)^{(p-1)/(p+1)} \times \exp\left[\frac{2.84(p + r)}{p + 1}\right], \quad (7)$$

$$r = 0.7 \ln\left[\frac{R_{\rm obs}(\epsilon, \nu)}{1.11 \times 10^{-8}}\right], \quad (8)$$

where $R_{\rm obs}(\epsilon, \nu)$ is the observed ratio of the fluxes. Using the observed flux ratios from Coma at several values of ϵ and ν, we find that for $p = 3$ the field strength is $B_\perp = 0.18$ μG. The required value of $B_\perp$ increases with p monotonically but slowly. For example, for $p = 5$ we find $B_\perp = 0.8$–0.3 μG depending on the values of ϵ and ν. This indicates that magnetic fields of about 1 μG may be possible if the electron spectrum steepens at some energy just below that needed for production of HXRs.

The energy ranges of electrons needed for production of observed HXR (20–80 keV), EUV (0.07–0.4 keV), and radio (0.03–3 GHz) fluxes are

$$0.53 < \frac{E_{\rm HXR}}{10^4} < 1.2 , \quad (9)$$

$$0.3 < \frac{E_{\rm EUV}}{10^3} < 0.75 , \quad (10)$$

$$0.4\left(\frac{\mu\text{G}}{B_\perp}\right)^{1/2} < \frac{E_{\rm rad}}{10^4} < 4\left(\frac{\mu\text{G}}{B_\perp}\right)^{1/2} . \quad (11)$$

Note that radio waves with $\nu > 0.35$ GHz are emitted by electrons above the range needed for the other emissions. Thus, a steepening of the accelerated electron spectrum at $E = E_{\rm cr} \sim 10^4$ will reduce the radio flux and allow a higher magnetic field. For example, if the spectral index of the electrons changes from 3 to 5 at $E_{\rm cr}$ (as in the Rephaeli 1979 model), then following equations (6) and (7), it can be shown that we need $B_\perp \simeq 0.5$ μG $(E_{\rm cr}/10^4)^{-2}$. Even higher magnetic fields will be allowed if the electron spectrum cuts off exponentially, as is the case for some acceleration models described by Schlickeiser et al. (1987; see also below). For $N(E) = N_0(E/E_{\rm cr})^{-p} \exp(-E/E_{\rm cr})$, the radio flux at high frequencies is reduced approximately by a factor of $(p - \frac{1}{3})E_{p+2/3}[(\nu/\nu_{\rm cr})^{1/2}]$, where $\nu_{\rm cr} = 0.42$ GHz$(B_\perp/\mu\text{G})(E_{\rm cr}/10^4)^2$ and $E_n(x)$ is the exponential integral function [this result is obtained by approximating the monoenergetic synchrotron spectrum as $\eta(\nu, E) = A(\nu/\nu_c)^{1/3}$ for $\nu \leq \nu_c = 3E^2\nu_B/2$]. Schlickeiser et al. (1987) show that a power-law spectrum with an exponential cutoff at $\nu_{\rm cr} = 0.15$ GHz provides a much better fit than a single or a double power-law model. With this cutoff frequency the application of the above correction factor yields $B_\perp \simeq 1.7$ and 1.1 μG for $p = 3$ and 4, respectively. These higher field strengths are in better agreement with the Faraday rotation measures quoted above.

We will return to these considerations in §§ 3.3 and 3.4 and show that these requirements set further constraints on the acceleration mechanism.

3.2.3. *Anisotropic Pitch Angle Distribution*

The gyroradius of the nonthermal electrons $r_g = 2\pi c\beta\gamma/\nu_{B_\perp} \sim 10^{11}$ cm $[\beta\gamma(\mu\text{G}/B_\perp)]$ is much smaller than all other relevant scales in clusters. Therefore, the electrons are attached to the field lines, and their distribution can be described by a gyrophase averaged distribution $N(E, \psi)$ as a function of energy and pitch angle ψ. In the above discussion we have implicitly assumed an isotropic pitch angle distribution. Anisotropies can modify some of the results quoted above. Note that all values of magnetic field are quoted in terms of $B_\perp$. For an ordered field and isotropic pitch angle distribution, the synchrotron emissivity is related to the component of the field perpendicular to the line of sight. However, as stated above, the magnetic field, even though ordered on scales comparable to and larger than r_g, must be chaotic on a kiloparsec scale. The emissivity averaged over scales larger than 1 kpc will be isotropic independent of any anisotropies in the monoenergetic emissivities and the pitch angle distribution. However, the overall intensity will depend on the pitch angle distribution. In this case $B_\perp = B \sin\psi$. The synchrotron emissivity at a given frequency is proportional to $B_\perp^{(p+1)/2}$ so that the above field values must be corrected by the value of $(\sin\psi)^{(p+1)/2}$ averaged over the pitch angle distribution in the range $0 < \psi < \pi/2$. If the distribution is isotropic, the average values of this quantity are $\frac{2}{3}$ and $\frac{8}{15}$ for $p = 3$ and 7, respectively, so that the actual values of magnetic field will be 1.5–2 times larger than those quoted above and could be as high as $B = 3$ μG.

Even higher fields will be required if the pitch angle distribution is anisotropic and is beamed along the field lines. For a Gaussian pitch angle distribution of width $\psi_0 < 1$ the field strengths increase by a factor of ψ_0^{-q}, where the value of q depends on several factors but is greater than 1 and could be as high as a few. The spectral shape also deviates from the usual power law with index $\alpha_{\rm synch} = (p - 1)/2$ depending on the values of ψ_0 and $\psi_0\gamma$. For further details on this see Epstein (1973) and Epstein & Petrosian (1973). Whether the acceleration mechanism will accelerate $E > 10^4$ electrons preferentially along a jumbled field line depends on the conditions in the background plasma. We will return to this in § 4 where we will argue in favor of the isotropic distribution.

In summary, there does not appear to be an insurmountable discrepancy between the field strengths required by the IC model for HXRs and the observed values.

3.3. *EUV Emission and Electron Spectral Index*

If the EUV emission is also produced by the IC process, the nonthermal electron distribution must extend to less than 100 MeV. Unfortunately, the electron spectral shape in this range is not well determined, and we must rely on the extrapolation of the spectra from the 10^4 MeV range, which can lead to a large uncertainty.

As already alluded to in § 3.2, there has been considerable discussion of the radio spectrum and its implications for the electron spectrum. A single power-law fit gives a value of radio spectral index of about $\alpha_{\rm synch} = 1.5$, implying an electron spectral index of $p = 4$. However, as pointed out by Schlickeiser et al. (1987), broken power laws provide a better fit. For example, the fit to the Rephaeli (1979) model yields a spectrum with index of about 1, which steepens to 2 above 0.6 GHz, implying electron spectral indices of $p = 3$ and $p_h = 5$, respectively, below and above the break energy of $E = 1.6 \times 10^4(\mu{\rm G}/B_\perp)^{1/2}$. An even better fit is obtained for a spectrum with an exponential cutoff $\eta(\nu) \propto \nu^{-0.52} e^{-(\nu/0.15\ {\rm GHz})^{1/2}}$, which means an index of $p = 2$. However, the range of the acceptable low-frequency spectral indices is fairly large. For the last model the 90% confidence range of $\alpha_{\rm synch}$ extends from 0.3 to -1.0, implying $-\infty < p < 3$ (see Schlickeiser et al. 1987).

The HXR spectrum is even more uncertain. Fusco-Femiano et al. (1999) give photon index $0.7 < \alpha < 3.6$, which allows $0.4 < p < 6$. Rephaeli et al. (1999) give a similar value but a smaller range of $1.9 < \alpha < 2.8$ so that $2.8 < p < 4.6$. The EUV observation when fitted to a power law indicates a photon spectral index in the range 1.3–2.0. If the EUV emission is also due to the IC process, these values of the photon index indicate a low-energy ($10^2 < E < 10^3$) electron index in the range $1.6 < p < 3.0$. For a summary of these observations see Table 1.

It therefore appears that a value of $p \lesssim 3$ is consistent with most of the data. A value of $p = 3$ implies an IC photon spectrum $f(\epsilon) \propto \epsilon^{-2}$ and equal energy emission per decade. The ratio of the observed EUV flux in the 0.07–0.4 keV range of 1.5×10^{-11} to the HXR (20–80 keV) flux of 2.2×10^{-11} ergs cm^{-3} s^{-1} (see Lieu et al. 1999; Fusco-Famiano et al. 1999) would indicate $p \sim 2.9$, which is also consistent with the above values.

In summary, the EUV, HXR, and radio data can be fitted by the IC and synchrotron emission in a chaotic magnetic field of strength around 1–2 μG by electrons with the same spectral distribution as that needed for the production of the observed radio spectrum via the synchrotron process.

3.4. *Spectrum of Radiating Electrons*

From the above discussions we can constrain the instantaneous spectrum of the radiating electrons as follows. We will assume an isotropic pitch angle distribution.

The radio and HXR observations indicate the presence of a power-law electron spectrum with an index $p < 3$ and sharp (preferably exponential) cutoff at $E > E_{\rm cr} \simeq 10^4(\mu{\rm G}/B_\perp)^{1/2}$. If the EUV emission is also due to the IC process, the electron spectrum must extend to about 100 MeV with a somewhat lower spectral index ($p \simeq 2.8$). At this energy about half of the electron energy is lost through Coulomb collisions and about 10% is radiated as bremsstrahlung photons of $\epsilon < 100$ MeV. Below $E = 200(10^{-3}\ {\rm cm}^{-3}/n)$ the collision losses become dominant, and for $E \le 10(10^{-3}\ {\rm cm}^{-3}/n)$ bremsstrahlung surpasses all other emissions. Therefore, there is a limit of how far this spectrum can be extended. It can easily be shown that if the electron spectrum is extended below 20 MeV with $p = 3$, the collisional heating rate of the background thermal plasma will exceed the rate of SXR TB emission. Since there are other sources of heating of the plasma, the electron spectrum must cut off rapidly at this or a higher energy. However, if the spectral change occurs at a higher energy, the cutoff does not necessarily have to be so severe. For example, a spectral break at $E_{\rm min} \sim E_p \simeq 200$ MeV with index $p_l \le 0.5$ can be extended to very low energies without violating the heating rate threshold. Note that in any case the NTB emission in the hard X-ray (20–80 keV) as well as gamma-ray ($\gtrsim$10 MeV) range will be negligible compared to the observed HXR flux. It can reach at most about 10% of the total losses at 200 MeV. Note also that the commonly used spectrum, which is a power law in terms of Lorentz factor γ (see, e.g., Giovannini & Feretti 2000), has a natural break (flattening) below 0.5 MeV. Such a spectrum also must flatten much before below $\gamma \sim 100$ to avoid the violation of the above-mentioned threshold.

There has been some discussion (see Bykov, Bloemen, & Uvarov 2000; Sarazin 2000) of a possible constraint imposed by the observed EGRET upper limit of $\sim 6 \times 10^{-12}$ ergs cm^{-2} s^{-1} above 100 MeV (Sreekumar et al. 1996), which is about 0.3 of HXR and 0.6 of EUV fluxes. This constraint is not very stringent because the expected bremsstrahlung flux by electrons above this energy is about 30 times smaller than their EUV emission or the HXR emission by higher energy electrons (see Fig. 1).

In summary, the radiating electron spectrum can be described as

$$N(E) = N_0 \begin{cases} \left(\dfrac{E}{E_{\rm cr}}\right)^{-p} e^{-(E-E_p)/E_{\rm cr}}, & \text{if } E_p < E, \text{ for } p \lesssim 3\ , \\ \left(\dfrac{E}{E_p}\right)^{-p_l}\left(\dfrac{E_p}{E_{\rm cr}}\right)^{-p}, & \text{if } E < E_p\ , \text{ for } p_l \le 0.5\ . \end{cases} \tag{12}$$

In the next section we discuss the types of acceleration mechanisms and plasma conditions that can give rise to such a spectrum. However, the reader is reminded that all the results in this section, including the above equation, are applicable to Coma and only to other clusters with similar observational characteristics.

4. ELECTRON ACCELERATION

The above spectrum is not necessarily that of the accelerated electrons. It would be in the case of thin target emission when only a small fraction of energy is lost during the radiation process in the ICM, i.e., if $\tau_{\rm loss} > T_{\rm cross} \sim R/c\beta$. As discussed in connection to Figure 1, this would appear to be the case for electrons with 200 keV $< E <$ 200 GeV. However, we face two critical problems if the electrons escape the ICM in a timescale shorter than their loss times. The first is that this requires an unreasonably high amount of energy for acceleration of the electrons; electrons in the relevant energy range radiate less than 1% of their energy in the ICM. The second problem is that escaping electrons will

continue to produce IC photons outside the ICM and will give rise to EUV and HXR emission that extends well beyond the cluster boundary as determined by the TB and radio (halo) emissions. This is not what is observed, especially at EUV energies where the source has been resolved (see Bowyer & Berghöfer 1998). Consequently, all electrons must be trapped, by chaotic fields or turbulence, and lose all their energy in the ICM as in a thick target model. It is therefore the totality of the acceleration, scattering, and loss processes that determine the spectrum of the radiating electrons. In this section we discuss some general features of the acceleration process and the conditions that can give rise to the spectrum given by equation (12).

4.1. *General Features of Acceleration*

The trapping of the electrons requires that they undergo repeated deflections or scatterings such that their effective transport time across the cluster, which we will refer to as the escape time, $T_{\rm esc} = T_{\rm cross}(R/\lambda_{\rm scat}) > \tau_{\rm loss}$, where $\lambda_{\rm scat} = c\beta\tau_{\rm scat}$ is the scattering (or deflection) mean free path. For this to be true for EUV-emitting electrons ($E \gtrsim 200$ MeV) we need $T_{\rm esc} \gtrsim 3 \times 10^9$ yr or $R/\lambda_{\rm scat} \gtrsim 10^3$, i.e., we need more than a million random scatterings. This implies a mean scattering timescale $\tau_{\rm scat} \lesssim 3 \times 10^3$, which is more than 10^3 times shorter than the crossing time and much shorter than all other relevant times (see Fig. 1).

A secondary effect of the repeated scatterings is that the pitch angle distribution of the electrons will be isotropic. The short mean free path also means that HXR- and radio-emitting electrons traverse distances equal to 1/40 and 1/200 of the cluster radius within their lifetimes. Consequently, for a smooth diffuse source the acceleration must be occurring throughout the ICM with inhomogeneity scale smaller than a few kiloparsecs, or the resolution of the observation if it is larger. [It should be noted that one can impose an ad hoc energy-dependent scattering process with mean free path $\lambda_{\rm scat}(E) = R^2/\lambda_{\rm loss}(E)$ so that the effective range of all electrons is $\sim R$ and $T_{\rm esc}(E) = \tau_{\rm loss}(E)$; see below.] We are therefore dealing with essentially a homogeneous and isotropic situation in which case the general Fokker-Planck transport equation describing the gyrophase and pitch angle averaged spectrum, $f(E, t)$, of the accelerated electrons is simplified to

$$\frac{\partial f}{\partial t} = \frac{\partial^2}{\partial E^2}\,[D(E)f] - \frac{\partial}{\partial E}\,\{[A(E) - |\dot{E}_L|]f\} - \frac{f}{T_{\rm esc}(E)} + Q(E, t)\,. \quad (13)$$

Here $D(E)$ and $A(E)$ are the diffusion and systematic acceleration coefficients, $Q(E, t)$ is a source term, $\dot{E}_L$ is the sum of the loss terms given in equations (1)–(4), and $T_{\rm esc}(E)$ is the escape time (see, e.g., Park & Petrosian 1995).

For stochastic acceleration by turbulence, a second-order Fermi acceleration process, $D(E) = \beta^2 D_{pp}$ and $A(E) = [D(E)/E][d\ln D/d\ln E + (2 - \gamma^{-2})/(1 - \gamma^{-1})]$ describe the diffusive and systematic accelerations, where D_{pp} is the momentum diffusion coefficient. From these we can define energy diffusion and acceleration times $\tau_{\rm diff} = E^2/D$ and $\tau_{\rm ac} = E/A$. The escape time is related to the mean scattering time $\tau_{\rm scat} \sim D_{\mu\mu}^{-1}$, where $D_{\mu\mu}$ is the pitch angle diffusion coefficient; $T_{\rm esc} = T_{\rm cross}^2 D_{\mu\mu}$. For relativistic particles in resonant interaction with Alfvén or Whistler waves, for example, $\tau_{\rm ac} \sim (\beta/\beta_{\rm A})^2\tau_{\rm scat}$, where $c\beta_{\rm A}$ is the Alfvén velocity (for further details see, e.g., Hamilton & Petrosian 1992). For ICM conditions $\beta_{\rm A} \simeq 2.3 \times 10^{-4}$, which means $\tau_{\rm ac} \simeq 10^7\tau_{\rm scat}$. For an efficient acceleration we need an acceleration time that is shorter than both the escape and the energy loss times. For the relevant energies this means $\tau_{\rm ac} \lesssim 10^8$ yr, $\tau_{\rm scat} \lesssim 10$ yr, and $T_{\rm esc} \gtrsim 10^{12}$ yr. Such a short scattering time may seem unreasonable but is possible. Very roughly this time is about $[\Omega_e(m_e/m_p)^{q-1}f_{\rm turb}]^{-1}$, where $\Omega_e \sim 20(B_\perp/\mu{\rm G})$ is the electron gyrofrequency, q is the spectral index of turbulence energy density, and $f_{\rm turb}$ is the ratio of the total turbulence energy density to the energy density of the magnetic field. A Kolmogorov index of 5/3 and $f_{\rm turb} \sim 10^{-6}$ would give a $\tau_{\rm scat}$ of approximately a few years, but a steeper spectrum will be less efficient and may require unreasonably large energy density for the turbulence (see also below). Figure 2 shows a comparison of these times with the total loss and crossing times from Figure 1.

The situation is very similar for acceleration by shocks, a first-order Fermi process, which also requires turbulence for scattering the electrons back and forth across the shock (see, e.g., Jones 1994). In this case we have the additional systematic acceleration term $A_{\rm sh}(E) \sim (\beta_{\rm sh}/\beta)^2 D_{\mu\mu}$, where the shock velocity $c\beta_{\rm sh}$ is of the order of the sound velocity. For ICM conditions $\beta_{\rm sh} \sim 3 \times 10^{-3}$ so that shock acceleration is about 100 times faster than stochastic acceleration. Hence, we require a 100 times longer scattering time, which requires correspondingly smaller density of turbulence. This and the corresponding escape time are also sketched in Figure 2.

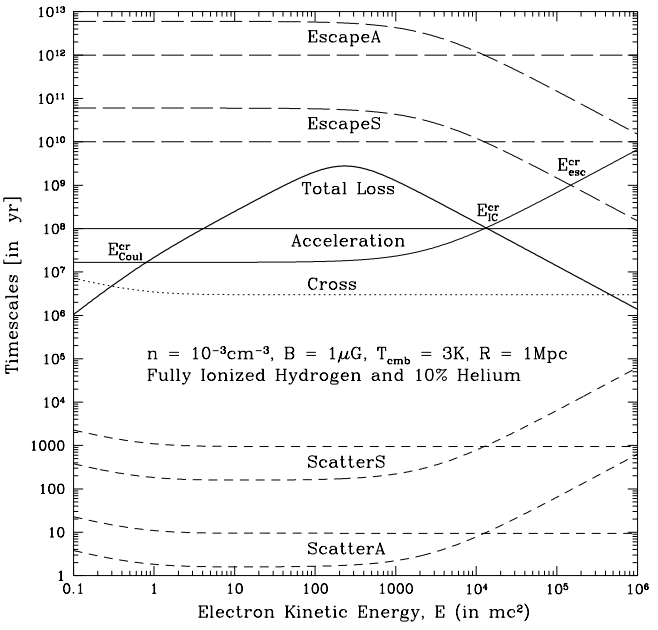

FIG. 2.—Comparison of the energy dependence of the "Total Loss" time (*thick solid line*; from Fig. 1) with timescales for scattering (*dashed line*), acceleration (*solid line*), and escape (*long-dashed line*) of electrons due to stochastic (A) and shock (S) acceleration for typical ICM conditions. Two examples are given: one with constant acceleration and other timescales, corresponding to an acceleration rate $A(E) \propto E$; and a second with variable timescales where $A(E) \rightarrow$ constant at high E, corresponding to an exponent $q = q' = 1$. The dotted line shows the average crossing time $T_{\rm cross} \sim R/(c\beta)$ across a region of size $R \sim 1$ Mpc. The critical energies, where the E-dependent acceleration time is equal to the escape time, and the Coulomb and IC loss times are shown.

We should, however, note that in general these timescales are energy dependent. For the cases discussed above one expects these times to vary as E^{2-q} (see Pryadko & Petrosian 1997). An example of energy-dependent timescales (with $q = 1$) is also shown in Figure 2. Note that with increasing scattering time the distance diffused by electrons increases and reduces the above-mentioned difficulty with the spatial smoothness of the acceleration process. However, for a complete removal of this difficulty we need $q = 1$ and $\tau_{\rm scat} \propto E^2$. We now consider several scenarios with opposing and somewhat extreme assumptions.

4.2. *Continuous Acceleration and Steady State Models*

The age of the GHz radio-emitting electrons ($E \sim 10^4$) could be as low as 10^8 yr (see Fig. 1 or Fig. 2) so that unless the observed nonthermal emission is a short transient event of comparable timescale we require a continuous acceleration or injection of nonthermal electrons in the ICM. In this case $Q(E, t)$ is a constant independent of time, and if the density and magnetic field change slowly, say, on a Hubble timescale like the CMB photons, then on this and shorter timescales we will be dealing with a time-independent or steady state situation with $\partial f/\partial t = 0$. Then $f(E)$ obtained from equation (13) represents the radiating electrons and must conform to equation (12).

4.2.1. *Acceleration of Thermal Electrons*

The most likely source for the accelerated electrons might appear to be the background hot plasma, $Q(E) = (\pi^{1/2}/2) n E_{\rm th}^{-3/2} E^{1/2} e^{-E/E_{\rm th}}$, where $E_{\rm th} = kT/m_e c^2 = 0.016$. However, this possibility suffers from two serious difficulties. The first has to do with the acceleration process. Although acceleration by plasma turbulence of low-energy (nonrelativistic) electrons is possible (Hamilton & Petrosian 1992), the required conditions for it are not the case in the ICM. Presence of short-wave [or high k vector, $k = 2\pi\nu_B/c \sim 6 \times 10^{-10}(B/\mu{\rm G})\ {\rm cm}^{-1}$] turbulence and a ratio of plasma to gyrofrequency of less than 1 [or Alfvén velocity $\beta_{\rm A} > (m_e/m_p)^{1/2} \simeq 0.023$] are required (see Pryadko & Petrosian 1997). In the ICM $\beta_{\rm A} \simeq 3 \times 10^{-4}$, and the value of this ratio is $100(n/10^{-3}\ {\rm cm}^{-3})^{1/2}(\mu{\rm G}/B) \gg 1$. Furthermore, it is not clear how such waves can be excited, and even if excited they will be damped quickly because of the high temperature of the ICM (Pryadko & Petrosian 1998, 1999).

The second and more serious difficulty in accelerating the background plasma electrons has to do with the high Coulomb losses (already encountered in § 3.1). The acceleration process must overcome the heavy losses the electrons will suffer as they are pulled from their low-energy state across the energy range from 10 keV to several hundred MeV. In addition, for a reasonable acceleration timescale, $\tau_{\rm ac} \sim 10^8$ yr, the accelerated electron spectrum will extend into the nonrelativistic region with a relatively steep upturn at $E \leq 0.5$, where $\tau_{\rm Coul} < \tau_{\rm ac}$ (see Hamilton & Petrosian 1992; Park, Petrosian, & Schwartz 1997). This does not agree with the desired equation (12), requires a high level of turbulence ($\sim 10^{48}$ ergs s^{-1}; see Blasi 2000), and will lead to the input of a high amount of energy in the ICM as in the NTB model. As discussed in § 3.1, this will heat up the ICM plasma to above 10^8 K in less than 10^8 yr. We therefore can conclude that the background thermal electrons cannot be the source for the nonthermal electrons, except for a short period of less than 10^8 yr.

4.2.2. *Acceleration of Injected Nonthermal Electrons*

To overcome both of the above difficulties, we require injection of relativistic electrons, presumably from the cluster galaxies, as the initial source. We first consider the simplest case of a delta function injection, $Q(E) = Q_0\,\delta(E - E_0)$. The acceleration process will distribute these electrons above and below E_0, and there could be other breaks at critical energies $E_{\rm Coul}^{\rm cr}$, $E_{\rm IC}^{\rm cr}$, and $E_{\rm esc}^{\rm cr}$, where the acceleration time $\tau_{\rm ac} = \tau_{\rm Coul}$, $\tau_{\rm IC}$, and $T_{\rm esc}$, respectively. Examples of these energies are shown in Figure 2. For a detailed discussion the reader is referred to Petrosian (1994) and Park & Petrosian (1995) and for some examples of complex spectra to Petrosian & Donaghy (1999). Here we describe some of the possibilities relevant to the problem at hand.

Although in certain circumstances the resultant spectrum can be approximated by a power law, this is the exception rather than the rule. A power-law spectrum over a wide range of energies is achieved for simple diffusion coefficients and for negligible losses. For example, for the simple case of

$$D(E) = \mathscr{D}E^{q'}\,, \quad A(E) = a\mathscr{D}E^{q'-1}\,, \quad T_{\rm esc} = \frac{E^s}{\theta\mathscr{D}}\,, \quad (14)$$

and for the special case of $s = 2 - q'$ one gets

$$N(E) \propto Q_0 \begin{cases} \left(\dfrac{E}{E_0}\right)^{a-x+(x^2+\theta)^{1/2}}, & \text{if } E < E_0\,, \\ \left(\dfrac{E}{E_0}\right)^{a-x-(x^2+\theta)^{1/2}}, & \text{if } E > E_0\,, \end{cases} \quad (15)$$

where $x = (a - 1 + q')/2$. Here we follow the notations of Pryadko & Petrosian (1997) and Petrosian & Donaghy (1999), rather than those of Park & Petrosian (1995) and Park et al. (1997), who use q for our q' here. In what follows we assume $E_0 < 200$ MeV and concentrate on the spectrum above E_0.

For $\theta \gg a \sim 1$, above E_0, $N \propto E^{-\theta^{1/2}}$. This is the kind of acceleration model used by Schlikeiser et al. (1987). If $s \neq 2 - q'$, the spectrum will deviate from a power law (exponentially as in modified Bessel functions I_n and K_n) at the energy $E_{\rm esc}^{\rm cr} \sim \theta^{1/|s-2+q'|}$. This may appear to be a good explanation for the exponential cutoff needed in equation (12) if $E_{\rm esc}^{\rm cr} \sim 10^4$. However, this would require $T_{\rm esc} \ll \tau_{\rm IC}$ below this energy, which, as stressed above, is ruled out by observations and arguments based on the energy budget. As shown in Figure 2 for the two acceleration models $\theta \sim \tau_{\rm ac}/T_{\rm esc} \sim 10^{-2}$ or 10^{-4} so that $E_{\rm esc}^{\rm cr} \gg 10^4$. In addition, because acceleration by shocks (if these exist in the ICM) is more efficient than by turbulence, the ratio of the systematic acceleration rate to the diffusion rate $a = (\tau_{\rm diff}/\tau_{\rm ac}) \sim \beta_s/\beta_{\rm A} \sim 10^2$. In this case, i.e., in the limit $\theta \to 0$, equation (15) reduces to

$$N(E) \propto Q_0 \begin{cases} \left(\dfrac{E}{E_0}\right)^{a}, & \text{if } E < E_0\,, \\ \left(\dfrac{E}{E_0}\right)^{-q'+1}, & \text{if } E > E_0\,, \end{cases} \quad (16)$$

so to obtain the index $p = 3$ required in equation (12) we need $q' = 4$. In general q' is related to the spectral index q describing the distribution of the wavevector of the turbulence. For Alfvén waves $q' = q$ so that we require a spectrum of turbulence that is much steeper than the commonly

assumed value of 5/3 expected for a Kolmogorov spectrum. As described in § 4.1, a high value of q will require a high level of turbulence, especially for the stochastic acceleration model.

A more reasonable explanation of the required exponential cutoff comes from inclusion of the losses in equation (13). As mentioned above, deviation from a power law is expected at energy $E_{\rm loss}^{\rm cr}$, where a specific loss time is equal to the acceleration time. The deviation occurs in the side where loss time is shorter. If $\tau_{\rm loss} < \tau_{\rm ac}$ for $E > E_{\rm loss}^{\rm cr}$ (assume to be greater than E_0), then the spectrum decreases sharply (approximately exponentially) above this energy. This situation can arise from IC and synchrotron losses if the acceleration time decreases more slowly than the loss time ($\propto E^{-1}$) as in the two examples shown in Figure 2. This requires a systematic acceleration rate of $A(E) \propto E^{<2}$, which for scattering by Alfvén waves (in either the stochastic or shock acceleration case) implies $q = q' < 3$. As evident from equation (16), this would give rise to an accelerated electron spectral index $p < 2$, which is too small. (For the constant and variable acceleration timescales shown in Figure 2, $q' = 2$ and 1, and $p = 1$ and 0, respectively.) In the opposite case of $q' > 3$, the loss time $\tau_{\rm loss} < \tau_{\rm ac}$ below $E_{\rm loss}^{\rm cr}$ and the spectrum steepens (becomes softer). This situation clearly cannot produce the exponential cutoff at high energies and may arise as a result of Coulomb losses at low (perhaps nonrelativistic) energies $E < E_{\rm Coul}^{\rm cr}$. For a thorough discussion of all possibilities see Park & Petrosian (1995).

Some of the above discussion is based on analytic solutions that are obtained for simple diffusion coefficients. In general these coefficients are more complex (Dung & Petrosian 1994; Pryadko & Petrosian 1997), and the resultant electron spectra could have other features such as a plateau just before the exponential cutoff (Park & Petrosian 1995; Petrosian & Donaghy 1999). Testing these more realistic models is beyond the scope of this paper and not warranted by the existing observations.

In summary, we can conclude that an exponential spectral cutoff can be produced at $E \sim 10^4$ if above this energy either $T_{\rm esc} < \tau_{\rm loss}$ or $T_{\rm esc} > \tau_{\rm loss}$ but $\tau_{\rm ac} < \tau_{\rm loss}$. The first possibility is ruled out by observations, and the second will give rise to a flat electron spectrum with $p \sim 1$. Although the existing radio, HXR, and EUV data do not have sufficient spectral resolution to rule out this model, a value of $p = 1$ is barely acceptable. Such a flat spectrum will also exacerbate the problem of a low required value for B. More importantly, if the EUV radiation is also due to the IC process, then the implied photon spectral index of $\alpha = (p + 1)/2 = 1$ would mean an HXR-to-EUV flux ratio of $(80 - 20)/(0.4 - 0.07) = 200$, which is more than 2 orders of magnitude larger than the observed value of less than 2. We note, however, that one can specify a contrived and unphysical energy dependence of the acceleration rate that can steepen the spectrum below 1 GeV to produce more EUV photons. We will not discuss such possibilities.

The above difficulty cannot be circumvented even if the injected electron spectrum, instead of being narrow as a delta function, is a broad power law: $Q(E) \propto E^{-p_0}$ for $E > E_{\rm min}$. In this case the final spectrum is obtained by the convolution of $Q(E' - E)$ with the above spectra. If we use the model of equation (16), for $p_0 > q' - 1$ this convolution will have no effect above $E_{\rm min}$ and the difficulty remains. But in the opposite case, $p_0 < q' - 1$, the acceleration process will have a negligible effect and the resultant spectrum will be essentially the same as the injected spectrum, which is now even flatter. Thus, we conclude that the steady state acceleration in the ICM of either thermal or nonthermal electrons cannot produce the requisite spectrum for reasonable physical conditions.

4.2.3. *Transport Effects and Cooling Spectra*

Considering the difficulties with the acceleration in the ICM discussed above, we now explore the possibility that electrons are accelerated somewhere else, presumably in galaxies, and are injected into the ICM, where they undergo only scattering and losses. In this case we still need some kind of turbulence to scatter and trap the electrons in the ICM, but we assume that these only isotropize the electrons and diffuse them spatially but cause neither diffusion in energy nor acceleration. As before, the scattering rate determines the escape time in equation (13), where now we set $D(E) = A(E) = 0$. Because we are interested in relativistic electrons, we approximate the loss term in equation (13) as

$$\frac{\dot{E}_L(E)}{E_p} = \frac{1 + (E/E_p)^2}{\tau_0} , \tag{17}$$

where

$$\tau_0 = (4\pi r_0^2 cn \ln\Lambda)^{-1} = 6.3 \times 10^9 \left(\frac{10^{-3}\ {\rm cm}^{-3}}{n}\right) {\rm yr} ,$$

$$E_p \simeq \left[\frac{9}{8}\left(\frac{n \ln\Lambda}{u_{\rm ph} + B^2/8\pi}\right)\right]^{1/2} = 235 , \tag{18}$$

are approximately the loss time (multiplied by 2) and the energy where the "Total Loss" curve reaches its maximum (see Figs. 1 and 2). Here we have ignored the bremsstrahlung loss and the weak dependence on E of Coulomb losses at nonrelativistic energies. Solution of equation (13) will then give the effective spectrum of the radiating electrons (commonly referred to as a cooling spectrum) that must conform to equation (12). The term $Q(E)$ represents the average rate of injection of accelerated electrons, which in general will have a broad distribution. A reasonable (and convenient) form is a power law, $Q(E) = Q_0(E/E_p)^{-p_0}$, with the same low-energy constraints as those used in connection with equation (12). Because most of the energy of electrons with $E < 100$ MeV goes into heating the ICM, the rate of injection of energy below this value must be less than the SXR thermal luminosity. Therefore, as stated in § 4.2.2, the spectrum of the injected electrons must drop off sharply below 8 MeV or have a spectral index $p_l < 0.5$. It should also be noted that the sources of injection must be sufficiently numerous and have a distribution such that they can produce a surface brightness distribution that is as smooth as that observed at radio wavelengths.

It can then be shown that for a finite and perhaps energy-dependent $T_{\rm esc}$, the steady state solution of equation (13) is

$$N(E) = \dot{E}_L^{-1} e^{-x} \int_E^\infty Q(E) e^x dE ,$$

$$\text{with } dx = -\frac{dE}{T_{\rm esc} \dot{E}_L} . \tag{19}$$

This is a partially cooled spectrum and has a break at $x \sim 1$ or at energy $E_{\rm cr}$ where $T_{\rm esc} = \tau_{\rm loss}$. For $x \ll 1$ or $T_{\rm esc} \gg \tau_{\rm loss}$

one expects a fully cooled spectrum, and for the opposite limit, $T_{\rm esc} \ll \tau_{\rm loss}$, the spectrum is the same as the injected spectrum multiplied by $T_{\rm esc}$. For example, for $T_{\rm esc} = \mathscr{T}_{\rm esc}(E/E_p)^{\nu-1}$ and for energies above the maximum of the $\tau_{\rm loss}$ curve at about 100 MeV, where $\tau_{\rm loss} \propto E^{-1}$, a power-law injected spectrum (for $\nu > 0$ and $p_0 > 1$) gives

$$N(E) = Q_0 \begin{cases} \left(\dfrac{\tau_0}{\nu}\right)\left(\dfrac{E}{E_p}\right)^{-p_0-1+\nu}, & \text{if } E_{\rm cr} \ll E, \\ \mathscr{T}_{\rm esc}\left(\dfrac{E}{E_p}\right)^{-p_0-1+\nu}, & \text{if } E \ll E_{\rm cr}, \end{cases} \tag{20}$$

where $E_{\rm cr} = E_p(\nu\mathscr{T}_{\rm esc}/\tau_0)^{-1/\nu}$. Thus, for $p_0 \sim 3$, $\nu \sim 0$, and $T_{\rm esc} \simeq 0.02\tau_0$ we obtain a spectrum with a break at $E \sim 10^4$, in good agreement with the radio data (Rephaeli 1979 model). However, a large fraction of the $E < E_p$ electrons escape from the ICM, or more accurately from the turbulent confining region, with a flux of $F_{\rm esc}(E) \propto N(E)/T_{\rm esc}(E)$. As already pointed out above, this is in disagreement with the observations. This difficulty is even more severe for a narrow injected spectrum, e.g., a delta function.

For the more reasonable case of $T_{\rm esc} \gg \tau_{\rm loss}$, equation (19) reduces to the fully cooled spectrum of $N(E) = \dot{E}_{\rm loss}^{-1}\int_E^\infty Q(E)dE$. For a delta function injection at a high energy the spectrum of the radiating electrons will vary as $\dot{E}_{\rm loss}^{-1}$, which will be essentially constant up to 200 MeV and then decrease with a power-law index $p = 2$. This does not agree with equation (12). For a power-law injected spectrum $N(E) = [Q_0/(p_0 - 1)](E/E_p)^{-p_0}\tau_{\rm loss}$, where $\tau_{\rm loss}$ is given by the thick solid line in Figure 2. For $p_0 = 2$ this will agree roughly with the data but not with the more accurate model of equation (12) with a break at $E \sim 10^4$. One way to have such a feature is if the injected electrons obtain the imprint of the break at their sources. In this case, by substitution of equation (12) for N in equation (13) with $D = A = T_{\rm esc}^{-1} = 0$, we find the necessary injected steady state spectrum to be $Q(E) \propto E^{2-p}e^{(-E/E_{\rm cr})}[(2-p)/E - 1]$ at high energies and with a similar expression at lower energies. This of course is an ad hoc assumption and does not clarify the acceleration mechanism. Thus, unless there exists an arbitrary and contrived injected spectrum, we must conclude that the steady state injection and cooling model also fails to describe the observations adequately.

4.3. *Time-dependent Models*

The upshot of the discussion in the previous section is that a steady state acceleration in the ICM or modification of simple accelerated spectra by transport processes in the ICM fails to reproduce the general features of the required spectrum. We therefore consider time-dependent scenarios with time variation shorter than the Hubble time. In this case we consider solutions of the time-dependent equation (13). We start with the generic model of a prompt one-time injection of electrons with $Q(E, t) = Q(E)\delta(t - t_0)$. More complex temporal behaviors can be obtained by the convolution of the injection time profile with the solutions described below. Similar but somewhat different treatments of the following cases can be found in Sarazin (1999) and Brunetti et al. (2000).

4.3.1. *Transport Effects*

We first consider the transport effects in the ICM without any acceleration. In this case, the time-dependent equation (13), with $D = A = 0$, $T_{\rm esc}$ independent of time and energy and $\dot{E}_L$ constant in time, has the following formal solution:

$$f(E, t) = \frac{\exp(-t/T_{\rm esc})Q[E'(E, t)]\dot{E}_L[E'(E, t)]}{\dot{E}_L(E)}, \tag{21}$$

where $E'(E, t) = \tau^{\rm inv}[\tau(E) - t]$ and $\tau^{\rm inv}$ is the inverse function of

$$\tau(E) = \int_E^\infty \frac{dE}{\dot{E}_L(E)}. \tag{22}$$

Using equation (17) for $\dot{E}_L(E)$, we find $\tau(E)/\tau_0 = \pi/2 - \tan^{-1}(E/E_p)$, $\tau^{\rm inv}(x) = \coth x$, and $E'/E_p = [E/E_p + \tan(t/\tau_0)]/[1 - (E/E_p)\tan(t/\tau_0)]$, so for a power-law injection $Q(E) = Q_0(E/E_p)^{-p_0}$, the solution for $p_0 \geq 2$ becomes

$$f(E, t) = \exp\left(-\frac{t}{T_{\rm esc}}\right)Q_0\frac{[1 - (E/E_p)\tan(t/\tau_0)]^{p_0-2}}{\cos^2(t/\tau_0)[E/E_p + \tan(t/\tau_0)]^{p_0}}. \tag{23}$$

The solid lines in Figure 3 show the spectral evolution according to this equation for the specified parameters and for several times past the injection epoch. At early times the spectrum is a power law in the energy range $\tan(t/\tau_0) < E/E_p < 1/\tan(t/\tau_0)$, goes to zero at $E/E_p = 1/\tan(t/\tau_0)$, and is flat for $E/E_p < \tan(t/\tau_0)$. As is expected, the power law extends to $E \gtrsim 4 \times 10^4$ needed for radio production only for a short period of $\tau_0/100$, i.e., $\lesssim 10^8$ yr. The power-law portion disappears for $t > \pi\tau_0/4 \sim 5 \times 10^9$ yr, and we obtain a degenerate flat spectrum extending to E_p. Between this and $t > \pi\tau_0/2 \sim 10^{10}$ yr the cutoff moves to lower energies and the amplitude drops as $\tan^{p_0-2}(t/\tau_0)$. In addition, the spectrum decays exponentially on a timescale of $T_{\rm esc}$ so that we need $T_{\rm esc} > \tau_0$, which requires the presence of turbulence or chaotic fields. Such a turbulence can also acceler-

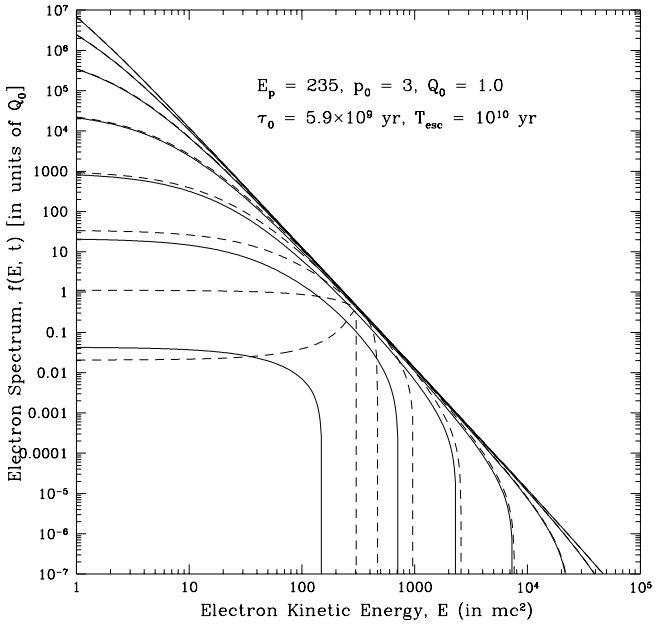

FIG. 3.—Evolution with time of a power-law injected spectrum (*top line*) subject to Coulomb and IC (plus synchrotron) losses as given by eq. (23) (*solid lines*; for times $t_n = 10^{n/2}\tau_0$, $n = -6$ to 0) and with acceleration ($b = 2$, $\delta = 0$) obtained from eq. (26) (*dashed lines*; for times $t_n = 10^{n/2}\tau_0$, $n = -6$ to 1).

ate the electrons. Therefore, the above spectra are correct if the acceleration time is longer than τ_0.

It is therefore clear that either the observable duration of the nonthermal activity in the clusters is a rare phenomenon or we need episodic injection of electrons on a timescale of 10^8 yr. Whether mergers and resulting shocks or AGN activities can provide such a source is unknown. If this is the case, then the rapid cutoff at $E/E_p = 1/\tan(t/\tau_0)$ may mimic the exponential form of equation (12) so that with $p_0 \lesssim 3$ this model will be acceptable.

4.3.2. *Acceleration plus Transport*

A more varied and complex set of spectra can be obtained if we add the effects of diffusion and acceleration. Simple analytic solutions for the time-dependent case are possible only for special cases. Most of the difficulty arises because of the diffusion term, which plays a vital role in shaping the spectrum for a narrow injection spectrum. For some examples see Park & Petrosian (1995). As we have seen for the steady state case, the effect of the diffusion is important for a narrow injected spectrum. Here we will limit our discussion to a broad initial electron spectrum in which case the effects of this term can be ignored. Thus, if we set $D(E) = 0$, then the solution (eq. [21]) of equation (13) can be generalized simply by inclusion of the systematic acceleration term $A(E)$ in $\dot{E}_L$ (see eqs. [14] and [17]) as

$$\frac{\dot{E}_L(E)}{E_p} = \frac{1 + (E/E_p)^2 - b(E/E_p)^{q'-1}}{\tau_0}, \tag{24}$$

where $b = a\mathscr{D}\tau_0 (E_p)^{q'} = \tau_0/\tau_{ac}(E_p) \sim 10^2$ or 1 for the shock or stochastic accelerations, respectively, and for the parameters described in § 4.3.1. For a general exponent q' one must resort to numerical solutions. For the purpose of demonstration of the effects of further ICM acceleration we consider the simple case of $q' = 2$ (corresponding to the constant acceleration timescale of Fig. 2), which has a solution similar to that shown by equation (23):

$$f(E, t) = \exp\left(-\frac{t}{T_{esc}}\right) Q_0 \times \frac{[T_+ - (E/E_p)\tan(\delta t/\tau_0)/\delta]^{p_0-2}}{\cos^2(\delta t/\tau_0)[T_-(E/E_p) + \tan(\delta t/\tau_0)/\delta]^{p_0}}, \tag{25}$$

where $\delta^2 = 1 - b^2/4$ and $T_\pm = 1 \pm b\tan(\delta t/\tau_0)/(2\delta)$. This solution (valid for $b^2 < 4$) reduces to that in equation (23) for $b = 0$. For $b^2 > 4$ we are dealing with an imaginary value for δ so that tangents and cosines become hyperbolic functions with $\delta^2 = b^2/4 - 1$. For $\delta = 0$ or $b = 2$ either form reduces to

$$f(E, t) = \exp\left(-\frac{t}{T_{esc}}\right) Q_0 \frac{[1 - (E/E_p - 1)t/\tau_0]^{p_0-2}}{[E/E_p - (E/E_p - 1)t/\tau_0]^{p_0}}. \tag{26}$$

The dashed lines in Figure 3 show the evolution of spectra for the latter case, and Figure 4 shows the solution according to equation (25) for larger values of b. As expected with acceleration, one can push the electron spectra to higher levels and extend them to higher energies, but as described below this does not significantly alter the above conclusion based on the transport effects alone, but it improves the situation somewhat.

For $b < 2$ the situation is similar to the case $b = 0$ (no acceleration) except that the spectra decay more slowly; the degenerate phase of a flat spectrum is reached later and extends to a higher energy. For $b > (2 + 4/p_0)^{1/2} \sim 1.83$ a local maximum appears during the degenerate phase just below the maximum energy (see Figs. 3 and 4). This peak could be very high and narrow. For $b > 2$ the acceleration becomes more and more important and can quickly reverse the decay and give rise to a growing spectrum. As before, for early times one gets a power-law spectrum at

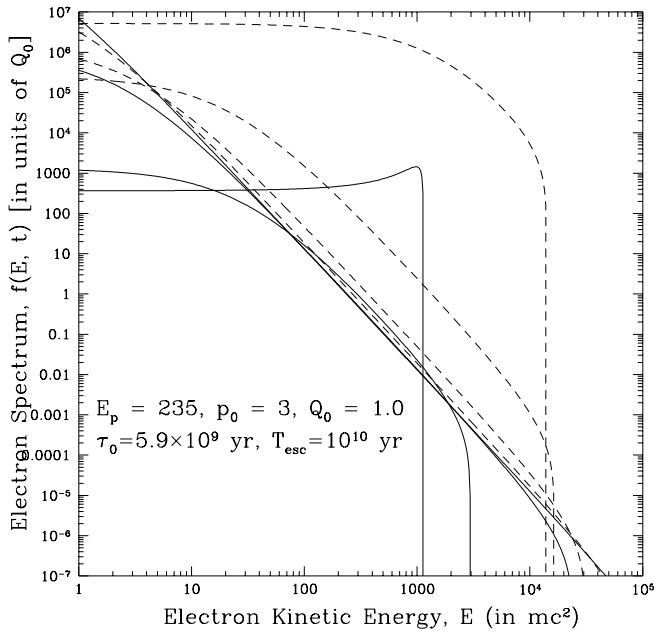

Fig. 4*a*

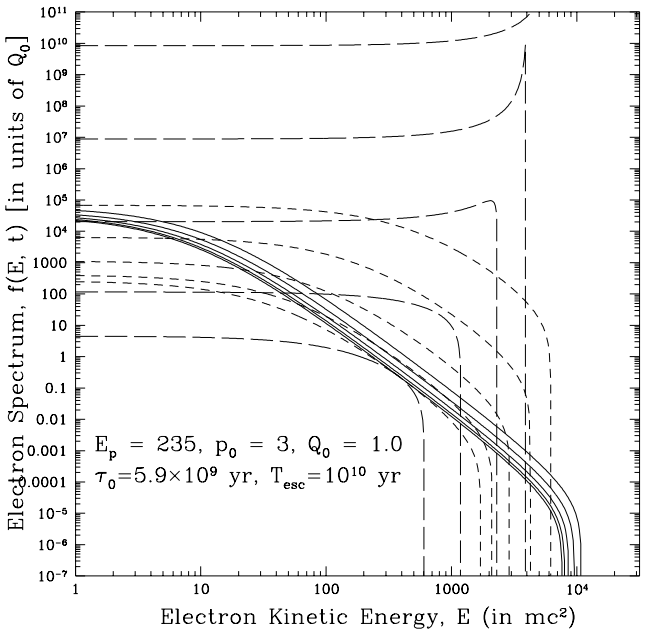

Fig. 4*b*

FIG. 4.—Same as Fig. 3, but for (*a*) $b = 5$ (*solid lines*; for $t/\tau_0 = 10^{-3}$, 10^{-2}, 10^{-1}, and 1) and $b = 60$ (*dashed lines*; for $t/\tau_0 c = 10^{-2.5}$, 10^{-2}, $10^{-1.5}$, and 10^{-1}); (*b*) $b = 2$, 5, 9, 17, and 26 (from lower to upper spectra) and at three different times, $t/\tau_0 = 10^{-1.5}$, $10^{-0.8}$, and $10^{-0.2}$ (*solid, dotted, and dashed lines*, respectively), obtained from eqs. (25) and (26).

$\tanh(\delta t/\tau_0)/(\delta T_-) < E/E_p < T_+ \delta/\tanh(\delta t/\tau_0)$. The spectrum now can be sustained to a high energy for all times:

$$\frac{E_{\max}}{E_p} = \frac{\delta + (b/2)\tanh(\delta t/\tau_0)}{\tanh(\delta t/\tau_0)} > \delta + \frac{b}{2} \simeq b\,. \qquad (27)$$

Thus, with faster acceleration rate (i.e., $b > 50$) we can have electron spectra extended above 10^4 MeV. However, the period when the spectrum below this energy is a power law is short. The degenerate phase is reached quickly when $\tanh(\delta t/\tau_0) = [\delta/(\delta + 2)]^{1/2}$. For large values of b this gives $t/\tau_0 = \ln\{\delta + 1 + [(\delta + 1)^2 + 1]^{1/2}\}/2\delta \rightarrow \ln(2\delta)/(2\delta)$, which is less than 5×10^8 yr for $b > 50$, implying a short duration for the power-law phase. As is evident from Figure 4, soon after the electrons are reaccelerated to above 10^4 MeV the power-law portion disappears. Of course, the situation can be improved with a more complex injected spectrum (e.g., a broken power law; see Brunetti et al. 2000) or with a time-dependent injection and/or acceleration parameters. However, some fine tuning may be required to sustain the required spectrum for a period significantly longer than 10^8 yr, which is essentially determined by the temperature of the CMB and the resultant lifetime of the $E = 10^4$ electrons. In any case the additional acceleration in the ICM improves the situation.

5. SUMMARY AND DISCUSSION

The purpose of this paper has been to investigate the emission mechanisms for the observed nonthermal radiation from the ICM of several clusters and to explore possible acceleration scenarios. We have used the observations of the Coma Cluster for our quantitative analyses. The qualitative aspects of the results summarized below are quite general, but the specific values of the parameters depend on the assumed values of the density, temperature, size, magnetic fields, etc., some of which are poorly known and can vary from cluster to cluster.

For the radiation mechanism, we have come to two important conclusions:

1. The source of the HXR flux cannot be NTB emission by semirelativistic electrons because of the extreme inefficiency of this process, unless it is a short-lived (less than 10^8 yr) phenomenon.

2. IC scattering of relativistic electrons by the CMB photons is a more natural process for production of both the HXR and EUV emissions. We have shown that the problems with a low value of magnetic field needed for this mechanism (discussed widely in the literature) can be alleviated when we include the effects of more realistic (broken power law) spectra and anisotropies in the pitch angle distribution of the electrons. Observational selection bias can also favor the IC emission at low magnetic fields.

Combining the requirements of the IC process for HXR and EUV emissions with the requirements of the synchrotron process for the radio emission, we derive a simple spectrum for the radiating electrons as described by equation (12).

Next we investigate the constraints that this spectrum and other considerations put on the acceleration mechanism. We consider both second-order Fermi stochastic acceleration by turbulence and first-order Fermi acceleration by shocks. We derive parameters for both these mechanisms so that they can accelerate electrons to the required energies of $E > 10^4$ MeV within their lifetime of 10^8 yr or shorter. The important conclusions here are the following:

1. The ICM must contain a high level of turbulence (or other scattering agent) to trap the electrons for time periods longer than their loss timescales and much longer than their crossing time across the cluster.

2. Acceleration of the thermal ICM electrons to relativistic energies will be difficult given the low value of the Alfvén velocity and more importantly requires input of a large amount of energy in the ICM. It will also give rise to an unacceptable spectrum for the IC model.

3. Steady state acceleration of injected relativistic electrons gives rise to a flatter spectrum than desired, or to an HXR and EUV source that extends well beyond the boundaries of the radio source.

4. Steady state cooling of a power-law injected spectrum also suffers from the same shortcoming or must involve ad hoc assumptions.

5. Time-dependent models fare much better. A power-law injected spectrum, under the influence of transport effects alone, can evolve into one with a high-energy cutoff at $E_{\rm cr} \sim 10^4$ (as required by the observations) after a time equal to the energy loss time at this energy, which is about 10^8 yr. For later times ($t > \tau_0 \sim 6 \times 10^9$ yr) the cutoff moves to lower energies and the spectrum becomes flat below it. If one adds an acceleration agent, then the spectrum can be maintained above the desired energy for a longer period. This requires an acceleration timescale that is shorter than 10^8 yr. However, at such high acceleration rates, the spectrum below this cutoff becomes flat in a shorter period of time, $t \sim \tau_0 \ln b/b$, where $b \sim \tau_0/\tau_{\rm ac}$. This can yield an acceptable spectrum for a period of about 5×10^8 yr.

The above results mean that either the nonthermal emissions from the ICM are short-lived and rare events or there is episodic injection of a power-law spectrum of relativistic electrons on a timescale of about 10^8 yr. This, however, still leaves the initial mechanism of the electron acceleration unresolved. A likely scenario is that episodic mergers of subclusters or encounters between galaxies can give rise to shocks and turbulence. The initial acceleration can take place in these shocks. The spectrum of radiating electrons is a result of transport and further acceleration (by turbulence) in the ICM. In such a situation, however, one would expect a different spatial distribution for the EUV emission than for HXR and radio emissions. The latter emitted by higher energy, shorter lived electrons will be more concentrated around the initial source. Similarly, a radial variation of the magnetic field could result in a more (or less) centrally concentrated synchrotron (radio) emission compared to the IC (HXR and perhaps EUV) emission. Density variations will affect mainly the bremsstrahlung emission relative to the other radiative processes but not the arguments based on the bremsstrahlung yield. Temperature variations can effect the spectrum of the turbulence.

An exact evaluation of the relative spatial distributions at different energy bands will require solution of an inhomogeneous Fokker-Planck equation, which in turn requires knowledge of energy and spatial dependences of scattering and escape processes, as well as spatial variation of density and magnetic field. This is beyond the scope of the present paper and not warranted by the existing observations.

Higher spatial resolution observation would be helpful here.

Alternative sites of the initial acceleration may be in galaxies, in which case the homogeneous model will be a good approximation. However, in this case, in addition to electrons one would expect a larger energy input in the form of protons. It is likely that protons may be the source of the turbulence that is essential for any viable model of nonthermal emission from the ICM.

This work was started while I was a visitor at the Institute For Advanced Studies and Bochum University. I would like to thank the support of both institutions and their staff and acknowledge stimulating discussions with J. N. Bahcall, P. Kumar, and R. Schlickeiser. I would also like to thank P. Blasi, A. M. Bykov, J. Eilek, T. A. Enßlin, and Y. Rephaeli for helpful discussions and several suggestions that led to the improvement of this paper.

REFERENCES

Atoyan, A. M., & Volk, H. J. 2000, ApJ, 535, 45
Berezinsky, V. S., Blasi, P., & Ptuskin, V. S. 1997, ApJ, 487, 529
Blasi, P. 2000, ApJ, 532, L9
Bowyer, S., & Berghöfer, T. W. 1998, ApJ, 506, 502
Brunetti, G., Setti, G., Feretti, L., & Gionannini, G. 2000, MNRAS, 320, 365
Bykov, A. M., Bloemen, H., & Uvarov, Yu. A. 2000, A&A, 362, 886
Dung, R., & Petrosian, V. 1994, ApJ, 421, 550
Eilek, J. 1999, Diffuse Thermal and Relativistic Plasma in Galaxy Clusters, ed. H. Boroinger, L. Feretti, & P. Schucker, MPr Rep. 271 (astro-ph/9906485)
Enßlin, T. A., & Biermann, P. 1998, A&A, 330, 90
Enßlin, T. A., Lieu, R., & Biermann, P. 1999, A&A, 344, 409
Epstein, R. I. 1973, ApJ, 183, 593
Epstein, R. I., & Petrosian, V. 1973, ApJ, 183, 611
Feretti, L., Dallacas, D., Giovannini, G., & Tagliani, A. 1995, A&A, 302, 680
Fusco-Femiano, R., Dal Fiume, D., Ferett, L., Giovannini, G., Grandi, P., Matt, G., Molendi, S., & Santangelo, A. 1999, ApJ, 513, L21
Fusco-Femiano, R., et al. 2000, ApJ, 534, L7
Giovannini, G., & Feretti, L. 2000, NewA, 5, 335
Giovannini, G., Feretti, L., Venture, T., Kim, K. T., & Kronberg, P. P. 1993, ApJ, 406, 399
Goldshmidt, O., & Rephaeli, Y. 1993, ApJ, 411, 518
Hamilton, R. J., & Petrosian, V. 1992, ApJ, 398, 350
Hwang, C.-Y. 1997, Science, 278, 1917
Jones, F. C. 1994, ApJS, 90, 561
Kaastra, J. S., Lieu, R., Mittaz, J. P. D., Bleeker, J. A. M., Mewe, R., Colafrancesco, S., & Lockman, F. J. 1999, ApJ, 519, L119
Kim, K. T., Kronberg, P. P., Dewdney, P. E., & Landecker, T. L. 1990, ApJ, 355, 29
Koch, H. W., & Motz, J. W. 1959, Rev. Mod. Phys., 31, 920
Lieu, R., Ip, W.-H., Axford, W. I., & Bonamente, M. 1999, ApJ, 510, L25
Lieu, R., Mittaz, J. P. D., Bowyer, S., Lockman, F. J., Hwang, C.-Y., & Schmitt, J. H. M. M. 1996a, ApJ, 458, L5
———. 1996b, Science, 274, 1335
Mittaz, J. P. D., Lieu, R., & Lockman, F. J. 1998, ApJ, 498, L17
Park, B. T., & Petrosian, V. 1995, ApJ, 446, 699
Park, B. T., Petrosian, V., & Schwartz, R. A. 1997, ApJ, 489, 358
Petrosian, V. 1973, ApJ, 186, 291
———. 1994, in AIP Conf. Proc. 294, High-Energy Solar Phenomena, ed. J. M. Ryan & W. T. Vestrand (New York: AIP), 162
Petrosian, V., & Donaghy, T. Q. 1999, ApJ, 527, 945
Pryadko, J., & Petrosian, V. 1997, ApJ, 482, 774
———. 1998, ApJ, 495, 377
———. 1999, ApJ, 515, 873
Rephaeli, Y. 1979, ApJ, 227, 364
Rephaeli, Y., Gruber, D., & Blanco, P. 1999, ApJ, 511, L21
Rybicki, G. B., & Lightman, A. P. 1979, in Radiation Processes in Astrophysics (New York: Wiley), 180 and 207
Sarazin, C. L. 1999, ApJ, 520, 529
———. 2000, Constructing the Universe with Clusters of Galaxies, ed. F. Durret & D. Gerbol, in press
Sarazin, C. L., & Kempner, J. C. 2000, ApJ, 533, 73
Sarazin, C. L., & Lieu, R. 1998, ApJ, 494, L177
Schlickeiser, R., Sievers, A., & Thiemann, H. 1987, A&A, 182, 21
Sreekumar, P., et al. 1996, ApJ, 464, 628